IJMMM International Journal of Minerals, Metallurgy and Materials
矿物冶金与材料学报（英文版）

First-principles calculations of Ni–(Co)–Mn–Cu–Ti all-d-metal Heusler alloy on martensitic transformation, mechanical and magnetic properties

Huaxin Qi, Jing Bai, Miao Jin, Jiaxin Xu, Xin Liu, Ziqi Guan, Jianglong Gu, Daoyong Cong, Xiang Zhao, and Liang Zuo

Cite this article as:
Huaxin Qi, Jing Bai, Miao Jin, Jiaxin Xu, Xin Liu, Ziqi Guan, Jianglong Gu, Daoyong Cong, Xiang Zhao, and Liang Zuo, First-principles calculations of Ni–(Co)–Mn–Cu–Ti all-d-metal Heusler alloy on martensitic transformation, mechanical and magnetic properties, *Int. J. Miner. Metall. Mater.*, 30(2023), No. 5, pp. 930-938. https://doi.org/10.1007/s12613-022-2566-5

International Journal of Minerals, Metallurgy and Materials
Volume 30, Number 5, May 2023, Page 930
https://doi.org/10.1007/s12613-022-2566-5

First-principles calculations of Ni–(Co)–Mn–Cu–Ti all-d-metal Heusler alloy on martensitic transformation, mechanical and magnetic properties

Huaxin Qi[1,2], *Jing Bai*[1,2),✉], *Miao Jin*[1,2], *Jiaxin Xu*[1,2], *Xin Liu*[1,2], *Ziqi Guan*[1], *Jianglong Gu*[3], *Daoyong Cong*[4),✉], *Xiang Zhao*[1], *and Liang Zuo*[1]

1) Key Laboratory for Anisotropy and Texture of Materials (Ministry of Education), School of Material Science and Engineering, Northeastern University, Shenyang 110819, China
2) Key Laboratory of Dielectric and Electrolyte Functional Material Hebei Province, School of Resources and Materials, Northeastern University at Qinhuangdao, Qinhuangdao 066004, China
3) State Key Laboratory of Metastable Materials Science and Technology, Yanshan University, Qinhuangdao 066004, China
4) Beijing Advanced Innovation Center for Materials Genome Engineering, State Key Laboratory for Advanced Metals and Materials, University of Science and Technology Beijing, Beijing 100083, China
(Received: 27 July 2022; revised: 21 October 2022; accepted: 25 October 2022)

Abstract: The martensitic transformation, mechanical, and magnetic properties of the $Ni_2Mn_{1.5-x}Cu_xTi_{0.5}$ (x = 0.125, 0.25, 0.375, 0.5) and $Ni_{2-y}Co_yMn_{1.5-x}Cu_xTi_{0.5}$ [(x = 0.125, y = 0.125, 0.25, 0.375, 0.5) and (x = 0.125, 0.25, 0.375, y = 0.625)] alloys were systematically studied by the first-principles calculations. For the formation energy, the martensite is smaller than the austenite, the Ni–(Co)–Mn–Cu–Ti alloys studied in this work can undergo martensitic transformation. The austenite and non-modulated (NM) martensite always present antiferromagnetic state in the $Ni_2Mn_{1.5-x}Cu_xTi_{0.5}$ and $Ni_{2-y}Co_yMn_{1.5-x}Cu_xTi_{0.5}$ (y < 0.625) alloys. When y = 0.625 in the $Ni_{2-y}Co_yMn_{1.5-x}Cu_xTi_{0.5}$ series, the austenite presents ferromagnetic state while the NM martensite shows antiferromagnetic state. Cu doping can decrease the thermal hysteresis and anisotropy of the Ni–(Co)–Mn–Ti alloy. Increasing Mn and decreasing Ti content can improve the shear resistance and normal stress resistance, but reduce the toughness in the Ni–Mn–Cu–Ti alloy. And the ductility of the Co–Cu co-doping alloy is inferior to that of the Ni–Mn–Cu–Ti and Ni–Co–Mn–Ti alloys. The electronic density of states was studied to reveal the essence of the mechanical and magnetic properties.

Keywords: Ni–Mn–Ti-based all-d-metal Heusler alloys; first-principles calculations; mechanical properties; martensitic transformation; magnetic properties.

1. Introduction

Shape memory alloys, such as Ni–Ti-based [1] and Ni–Mn-based Heusler alloys [2–4], are environmentally friendly and highly efficient, and are widely used in solid-state refrigeration [5], medical treatment [6], and aerospace [7]. Ni–Mn–Z-based (Z = Ga, In, Sn, etc.) Heusler alloys possess magnetic-field induced shape memory effect [8–11], larger magnetocaloric [12–14] and elastocaloric effect [14–16] during martensitic transformation (MT). However, intrinsic brittleness resulting from the p–d covalent hybridization between main group elements (Ni and Mn) and transitional element (Z) greatly limits its practical application. Wei *et al.* [17] found that the compressive strength of the novel $Ni_{50}Mn_{32}Ti_{18}$ all-d-metal Heusler alloy overtopped 900 MPa and the change of adiabatic temperature was 10.7 K under the 3.9% strain level. Yan *et al.* [18] found the 1.1 GPa maximum compressive strength and the 13% directionally solidified strain in the $Ni_{50}Mn_{31.75}Ti_{18.25}$ alloy. Due to the d–d hybridization among transition-metal elements in the Ni–Mn–Ti alloys, the mechanical properties of ternary Ni–Mn–Ti alloy were significantly improved compared with the conventional Ni–Mn-based alloys, but the magnetocaloric effect was absent because the magnetization difference (ΔM) between the austenite and martensite is almost zero.

Composition alloying is an effective method to enhance the MT and magnetic properties for the Ni–Mn–Ti alloy. Some researchers try to dope Co element in Ni–Mn–Ti alloy to enhance the magnetism. Wei *et al.* [19] found that under the 0.01 T magnetic field, the ΔM between martensite and austenite of the $Ni_{35}Co_{15}Mn_{35}Ti_{15}$ alloy can reach 15 emu·g^{-1}. Liu *et al.* [20] found that annealed $Ni_{36.5}Co_{13.5}Mn_{35}Ti_{15}$ alloy has a large magnetic entropy change of about 25 J·kg^{-1}·K^{-1} under a 5 T magnetic field. Guan *et al.* [21] found that the magnetization change and magnetic entropy change in the $Ni_{36}Co_{14}Mn_{35}Ti_{15}$ alloy under the magnetic field of 5 T reached 106 emu·g^{-1} and 19.3 J·kg^{-1}·K^{-1}, respectively. Researchers [22] proved that the magnetic entropy change of the

✉ Corresponding authors: Jing Bai E-mail: baijing@neuq.edu.cn; Daoyong Cong E-mail: dycong@ustb.edu.cn

$Ni_{37}Co_{13}Mn_{34}Ti_{16}$ alloy reached 38 $J \cdot kg^{-1} \cdot K^{-1}$ at 2 T magnetic field. The above results proved that Co doping can significantly improve ferromagnetism [23].

In this paper, the MT, mechanical and magnetic properties in Ni–(Co)–Mn–Cu–Ti alloys were studied according to the first-principles calculations, aiming to provide theoretical support for composition design.

2. Calculation methods

The Vienna *Ab-initio* Simulation Package (VASP) [24–25] was used for the first-principles calculations. The projector-augmented wave (PAW) [26–27] method described the interaction between ions and electrons and the Perdew–Burke–Ernzerhof implementation of generalized gradient approximation (GGA) [28] processed the exchange-correlation potential. The valence electronic states were Ni-$3d^8 4s^2$, Mn-$3d^6 4s^1$, Ti-$3d^2 4s^2$, Co-$3d^8 4s^1$, and Cu-$3d^{10} 4s^1$. The kinetic energy cutoff was 384 eV. The k-point mesh was generated using the Monkhorst–Pack grid [29] in the Brillouin zone and 10 × 10 × 5 and 7 × 7 × 11 k-points for the 32-atom austenite and NM martensite supercell were used, respectively. The convergence criteria for the total energies were smaller than 1 meV and the total and atomic forces were smaller than 0.2 eV/nm, respectively. The elastic constants were calculated by the stress–strain method. The formation energy (E_{form}) was calculated by Eq. (1).

$$E_{form} = \frac{E_{total} - N_{Ni} \times E_{Ni} - N_{Mn} \times E_{Mn} - N_{Ti} \times E_{Ti} - N_{Co} \times E_{Co} - N_{Cu} \times E_{Cu}}{N} \quad (1)$$

where E_{total} is the compound total energy and N is the total atomic number in the unitcell, and the N_i (i = Ni, Mn, Ti, Co, Cu) is the atomic number in the unitcell and E_i is the ground state energy per atom in its reference bulk state, respectively.

For easy expression, the abbreviations of AFA, FA, AFM, and FM were used to describe the antiferromagnetic austenite, ferromagnetic austenite, antiferromagnetic martensite, and ferromagnetic martensite, respectively. The abbreviations of $Ni_2Mn_{1.5-x}Cu_xTi_{0.5}$ (x = 0, 0.125, 0.25, 0.375, 0.5) and $Ni_{2-y}Co_yMn_{1.5-x}Cu_xTi_{0.5}$ [(x = 0.125, y = 0.125, 0.25, 0.375, 0.5) and (x = 0.125, 0.25, 0.375, y = 0.625)] alloys are shown in Table 1.

Table 1. Abbreviations of $Ni_2Mn_{1.5-x}Cu_xTi_{0.5}$ (x = 0, 0.125, 0.25, 0.375, 0.5) and $Ni_{2-y}Co_yMn_{1.5-x}Cu_xTi_{0.5}$ [(x = 0.125, y = 0.125, 0.25, 0.375, 0.5) and (x = 0.125, 0.25, 0.375, y = 0.625)] alloys

Component	$x = 0$	$x = 0.125$	$x = 0.25$	$x = 0.375$	$x = 0.5$	$y = 0.125$	$y = 0.25$	$y = 0.375$	$y = 0.5$
$Ni_2Mn_{1.5-x}Cu_xTi_{0.5}$	Cu0	Cu1	Cu2	Cu3	Cu4				
$Ni_{1.375}Co_{0.625}Mn_{1.5-x}Cu_xTi_{0.5}$		Cu1Co5	Cu2Co5	Cu3Co5					
$Ni_{2-y}Co_yMn_{1.375}Cu_{0.125}Ti_{0.5}$						Cu1Co1	Cu1Co2	Cu1Co3	Cu1Co4

3. Results and discussion

3.1. Phase stability and martensitic transformation

When doping a Cu atom in the supercell, the preferential site occupation of Cu should be considered. Cu substituting Ni, Mn, Ti sites are referred to as Cu_{Ni}, Cu_{Mn}, and Cu_{Ti}, respectively. The structural model and the corresponding E_{form} of the austenite for Cu_{Ni}, Cu_{Mn}, and Cu_{Ti} cases are shown in Fig. 1(a)–(c). The sequence of the formation energy is $Cu_{Mn} < Cu_{Ni} < Cu_{Ti}$, therefore, the doped Cu prefers to occupy the Mn sublattice.

When more Cu atoms are doped in a supercell, the effect of Cu–Cu distance should be considered. The doping Cu atoms are dispersive and aggregated distribution in the supercell that are represented by Cu2(D) and Cu2(A), respectively. The structural model and the corresponding E_{form} of the austenite for Cu2(A) and Cu2(D) cases of the doped Cu in the $Ni_2Mn_{1.25}Cu_{0.25}Ti_{0.5}$ alloy are shown in Fig. 1(d) and (e). The E_{form} of the Cu2(A) is much lower than that of the Cu2(D), which means doping Cu atoms prefer to be aggregated to reduce the total energy in the Ni–Mn–Cu–Ti alloy.

The E_{form} for the martensite and austenite of the $Ni_2Mn_{1.5-x}Cu_xTi_{0.5}$ (x = 0.125, 0.25, 0.375, 0.5) and $Ni_{2-y}Co_yMn_{1.5-x}Cu_xTi_{0.5}$ [(x = 0.125, y = 0.125, 0.25, 0.375, 0.5) and (x = 0.125, 0.25, 0.375, y = 0.625)] alloys is shown in Fig. 2. For the E_{form}, the antiferromagnetic state is always smaller than ferromagnetic state. It means that the alloys are always present antiferromagnetic state no matter austenite or martensite. While for E_{form} of the $Ni_{2-y}Co_yMn_{1.5-x}Cu_xTi_{0.5}$ (x = 0.125, 0.25, 0.375, y = 0.625) alloys, the antiferromagnetic martensite is always smaller than the ferromagnetic case, however, the E_{form} of the ferromagnetic austenite is always lower than that of antiferromagnetic one, which indicates that the austenite prefers to be ferromagnetic and the martensite tends to be antiferromagnetic.

Besides, for the E_{form}, the martensite is smaller than the austenite, so all the investigated Ni–(Co)–Mn–Cu–Ti alloys can undergo MT. The change of magnetism occurs during MT in the $Ni_{2-y}Co_yMn_{1.5-x}Cu_xTi_{0.5}$ (x = 0.125, 0.25, 0.375, y = 0.625) alloy system. It should be noted that the E_{form} increases with the increase in Cu content in the $Ni_{2-y}Co_yMn_{1.5-x}Cu_xTi_{0.5}$ (x = 0.125, 0.25, 0.375, y = 0.625) system, which means the stability of the martensite and austenite gradually reduces, but the austenite E_{form} of the Ni–Mn–Cu–Ti alloy decreases with doping Cu content, which reveals the increasing stability of the austenite.

The equilibrium lattice constants, volume, and volume change for the martensite and austenite for the $Ni_2Mn_{1.5-x}Cu_xTi_{0.5}$ and $Ni_{2-y}Co_yMn_{1.5-x}Cu_xTi_{0.5}$ systems are shown in Table 2. According to Table 2, the equilibrium lat-

tice constants of the austenite tend to decrease with the increase in Cu and Co content. The volume of the AFA and AFM phases of the $Ni_{2-y}Co_yMn_{1.375}Cu_{0.125}Ti_{0.5}$ (y = 0.125, 0.25, 0.375, 0.5) alloys generally reduces with the increase in Co content.

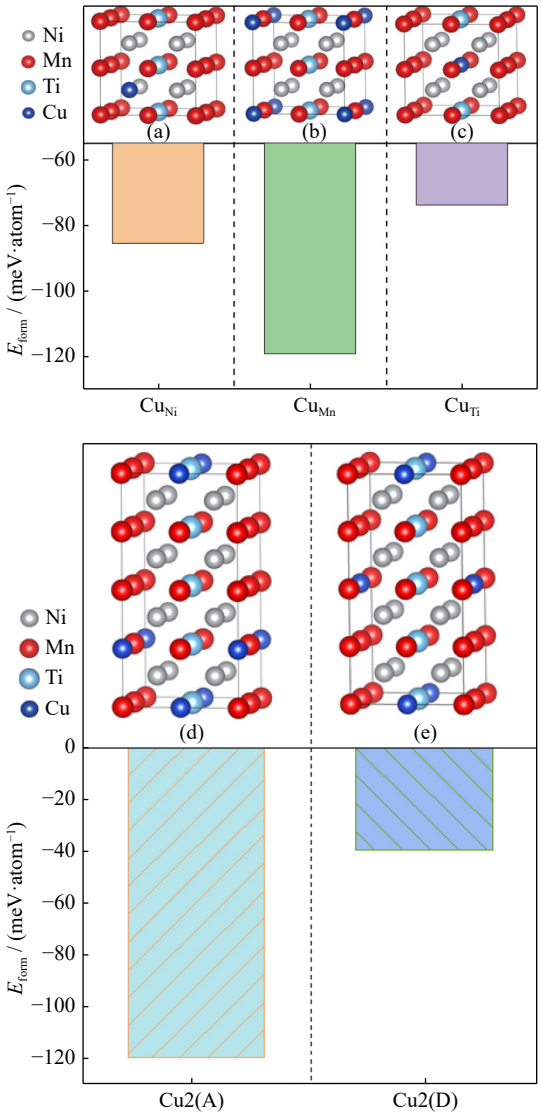

Fig. 1. Structural model and corresponding formation energy of Cu substituting (a) Ni, (b) Mn, and (c) Ti site in $Ni_2Mn_{1.5}Ti_{0.5}$ alloy; structural model and corresponding formation energy of (d) aggregated and (e) dispersive distribution of doped Cu atoms in $Ni_2Mn_{1.25}Cu_{0.25}Ti_{0.5}$ alloy.

The geometrical compatibility between the austenite and martensite has a great influence on the thermal hysteresis (ΔT_{Hys}) [30–31], and the ΔT_{Hys} can be qualitatively described by volume change (ΔV) [32]. Generally, the ΔT_{Hys} increases with the increasing ΔV. According to Table 2, the ΔV of the $Ni_2Mn_{1.5}Ti_{0.5}$ alloy is the largest. When doped with five Co atoms in the 32-atom $Ni_{2-y}Co_yMn_{1.5-x}Cu_xTi_{0.5}$ alloy, the magnetism of the austenite reverses, and the ΔV increases. The volume for FA decreases with doping Cu, but AFM increases, so the ΔV decreases. In addition, researchers [33–36] proved that Cu doping can reduce ΔT_{Hys}. Therefore, the Cu doping and Cu–Co co-doping can effectively reduce the ΔV and thus the ΔT_{Hys}.

In addition, the volume of austenite is always larger than that of the martensite phase, as shown in Table 2, which implies that the MT in the Ni–(Co)–Mn–Cu–Ti alloy is accompanied by volume contraction.

3.2. Mechanical and magnetic properties

The Young's modulus $Y = \frac{9BG}{3B+G}$, shear modulus $G = \frac{3C_{11}-3C_{12}+4C_{44}}{10}$, bulk modulus $B = \frac{C_{11}+2C_{12}}{3}$, and Poisson's ratio $\nu = \frac{3B-2G}{2G+6B}$ of the $Ni_2Mn_{0.75}Cu_{0.25}Ti$, $Ni_2MnCu_{0.25}Ti_{0.75}$, $Ni_2Mn_{1.25}Cu_{0.25}Ti_{0.5}$, $Ni_{1.5}Co_{0.5}MnTi$, and $Ni_{1.5}Co_{0.5}Mn_{1.25}Cu_{0.25}Ti_{0.5}$ alloys are obtained in the present work and the results are listed in Table 3. Guan *et al.* [37] calculated the elastic constants of the cubic austenite of the Ni_2MnTi, Ni_2MnIn, and Ni_2MnGa alloys, and Xiong *et al.* [38] calculated the elastic constants of the cubic austenite of the $(Ni_2MnTi)_{0.89}B_{0.11}$ alloys, these data are also listed in Table 3 for comparison.

The alloy can be classified as ductile material when the Pugh ratio $B/G > 1.75$ and Cauchy pressure $P_c = C_{12} - C_{44} > 0$. Compared with Ni_2MnIn and Ni_2MnGa alloys, $Ni_2Mn_{0.75}Cu_{0.25}Ti$, $Ni_2MnCu_{0.25}Ti_{0.75}$, $Ni_2Mn_{1.25}Cu_{0.25}Ti_{0.5}$, and $Ni_{1.5}Co_{0.5}MnTi$ alloys possess smaller G and Y values. The results show that Ni–Mn–Cu–Ti and Ni–Co–Mn–Ti alloys

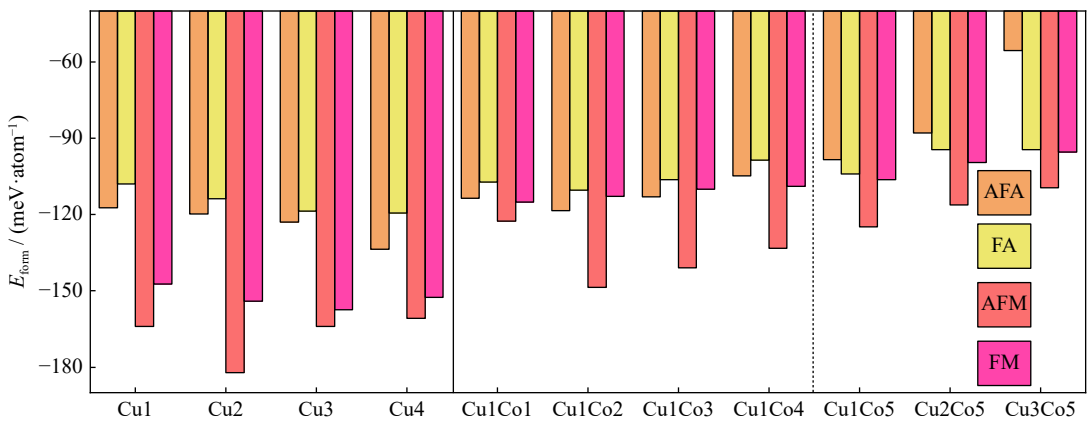

Fig. 2. Formation energy of austenite and martensite for $Ni_2Mn_{1.5-x}Cu_xTi_{0.5}$ (x = 0.125, 0.25, 0.375, 0.5) and $Ni_{2-y}Co_yMn_{1.5-x}Cu_xTi_{0.5}$ [(x = 0.125, y = 0.125, 0.25, 0.375, 0.5) and (x = 0.125, 0.25, 0.375, y = 0.625)] alloys.

Table 2. Equilibrium lattice constants, volume, and volume change of austenite and martensite for $Ni_2Mn_{1.5-x}Cu_xTi_{0.5}$ (x = 0, 0.125, 0.25, 0.375, 0.5) and $Ni_{2-y}Co_yMn_{1.5-x}Cu_xTi_{0.5}$ [(x = 0.125, y = 0.125, 0.25, 0.375, 0.5) and (x = 0.125, 0.25, 0.375, y = 0.625)] systems

Component	AFA		Non-modulated AFM				
	a / nm	Cell volume / nm^3	a / nm	b / nm	c / nm	Cell volume / nm^3	ΔV / nm^3
Cu0	0.58483	0.200027	0.89960	0.41761	0.51238	0.192492	0.007535
Cu1	0.58397	0.199146	0.86000	0.43085	0.52817	0.195703	0.003443
Cu2	0.58353	0.198696	0.84016	0.44325	0.51792	0.192874	0.005822
Cu3	0.58258	0.197727	0.87623	0.42103	0.52404	0.193328	0.004399
Cu4	0.58013	0.195243	0.86075	0.42927	0.52416	0.193674	0.001569
Cu1Co1	0.58369	0.198860	0.81653	0.40860	0.59234	0.197625	0.001235
Cu1Co2	0.58127	0.196396	0.74669	0.37374	0.69185	0.193073	0.003323
Cu1Co3	0.58123	0.196356	0.74698	0.37448	0.68892	0.192711	0.003645
Cu1Co4	0.58029	0.195405	0.74651	0.37483	0.68688	0.192199	0.003206
Component	FA		Non-modulated AFM				
	a / nm	Cell volume / nm^3	a / nm	b / nm	c / nm	Cell volume / nm^3	ΔV / nm^3
Cu1Co5	0.58309	0.198247	0.74685	0.37615	0.68292	0.191851	0.006396
Cu2Co5	0.58229	0.197432	0.75242	0.37926	0.67376	0.192266	0.005166
Cu3Co5	0.58108	0.196204	0.75695	0.38176	0.66582	0.192404	0.003800

Notes: a, b, and c are the side lengths of the cell along the x, y, and z axes, respectively.

Table 3. Elastic constants (C_{11}, C_{12}, and C_{44}), elastic modulus (bulk modulus B, shear modulus G, and Young's modulus Y), Cauchy pressure P_c, B/G ratio, and Poisson's ratio ν of $Ni_2Mn_{0.75}Cu_{0.25}Ti$, $Ni_2MnCu_{0.25}Ti_{0.75}$, $Ni_2Mn_{1.25}Cu_{0.25}Ti_{0.5}$, $Ni_{1.5}Co_{0.5}MnTi$, $Ni_{1.5}Co_{0.5}Mn_{1.25}Cu_{0.25}Ti_{0.5}$, $(Ni_2MnTi)_{0.89}B_{0.11}$, Ni_2MnTi, Ni_2MnGa, and Ni_2MnIn alloys. Elastic properties of Ni_2MnTi, Ni_2MnGa, and Ni_2MnIn alloy are cited from Ref. [37], elastic properties of $(Ni_2MnTi)_{0.89}B_{0.11}$ are cited from Ref. [38]

System	Mechanical property constants								
	C_{11} / GPa	C_{12} / GPa	C_{44} / GPa	B / GPa	G / GPa	Y / GPa	P_c / GPa	B/G	ν
$Ni_{1.5}Co_{0.5}Mn_{1.25}Cu_{0.25}Ti_{0.5}$	115.75	110.90	87.75	112.52	36.55	98.94	23.15	3.08	0.35
$Ni_2Mn_{0.75}Cu_{0.25}Ti$	132.35	130.63	82.20	131.20	33.39	92.34	48.44	3.93	0.38
$Ni_2MnCu_{0.25}Ti_{0.75}$	145.45	141.41	88.30	142.76	36.53	100.98	53.12	3.91	0.38
$Ni_2Mn_{1.25}Cu_{0.25}Ti_{0.5}$	140.29	139.98	95.18	140.08	38.17	104.98	44.80	3.67	0.38
$Ni_{1.5}Co_{0.5}MnTi$	153.06	145.01	83.74	147.69	35.91	99.65	61.27	4.11	0.39
$(Ni_2MnTi)_{0.89}B_{0.11}$ [38]	232.70	123.85	113.53	160.13	78.07	201.46	10.32	2.05	0.29
Ni_2MnTi [37]	153.89	146.14	77.27	148.72	33.23	92.78	68.87	4.48	0.40
Ni_2MnGa [37]	155.20	139.63	103.28	144.82	45.98	124.74	36.35	3.15	0.36
Ni_2MnIn [37]	150.89	132.76	95.95	138.81	43.82	118.94	36.81	3.17	0.36

have weaker shear resistance and normal stress resistance, but Ni–Co–Mn–Ti alloy possesses greater incompressibility. However, the Ni–Mn–Cu–Ti and Ni–Co–Mn–Ti alloys have a larger value of P_c, B/G, and ν than those of the Ni_2MnIn and Ni_2MnGa alloys, which is the essence for the enhancement of ductility and plasticity of the Ni–Mn–Ti-based alloys [18].

For the B, P_c, B/G, and ν, the Ni–Mn–Cu–Ti alloy is larger than the $Ni_{1.5}Co_{0.5}Mn_{1.25}Cu_{0.25}Ti_{0.5}$ alloy and the Ni_2MnTi alloy is larger than the $Ni_{1.5}Co_{0.5}MnTi$ alloy, which indicates that the Co doping reduces the incompressibility and ductility of the Ni–Mn–(Cu)–Ti alloy. While the $Ni_{1.5}Co_{0.5}MnTi$ alloy is larger than the $Ni_{1.5}Co_{0.5}Mn_{1.25}Cu_{0.25}Ti_{0.5}$ alloy and the Ni_2MnTi alloy is larger than the Ni–Mn–Cu–Ti alloy, which suggests that the Cu doping also reduces the incompressibility and ductility in the Ni–(Co)–Mn–Ti alloy.

The larger the P_c, B/G, and ν, the better the toughness. The P_c, B/G, and ν for the $Ni_{1.5}Co_{0.5}MnTi$ alloy are larger than that of the Ni–Mn–Cu–Ti alloy, the toughness of the $Ni_{1.5}Co_{0.5}MnTi$ alloy is better than that of the Ni–Mn–Cu–Ti alloy. Besides, doping Co in ternary Ni_2MnTi alloy presents magnetocaloric effect. Therefore, Co doping is beneficial for the alloy to obtain both magnetocaloric effect and has little effect on toughness [21,39].

With the increase of Mn content and the decrease of Ti content, the G and Y values increase, but B/G decreases, which indicates that the increasing Mn and decreasing Ti content can improve the shear resistance and normal stress resistance, but reduce the toughness in the Ni–Mn–Cu–Ti alloy.

Three-dimensional Young's modulus for the single-crys-

tal Ni_2MnTi, $Ni_{1.5}Cu_{0.5}MnTi$, $Ni_2Mn_{0.75}Cu_{0.25}Ti$, $Ni_{1.5}Co_{0.5}MnTi$, and $Ni_{1.5}Co_{0.5}Mn_{1.25}Cu_{0.25}Ti_{0.5}$ alloys is shown in Fig. 3. In Fig. 3, the anisotropy of the $Ni_{1.5}Co_{0.5}MnTi$ alloy is the strongest, which means that doping Co can increase the anisotropy of the Ni–Mn–Ti-based alloys. In addition, the anisotropy of Ni_2MnTi alloy can be reduced by doping Cu.

The total and atomic magnetic moments of the $Ni_2Mn_{1.5-x}Cu_xTi_{0.5}$ and $Ni_{2-y}Co_yMn_{1.5-x}Cu_xTi_{0.5}$ alloy systems are shown in Fig. 4. According to Fig. 4(a), the magnetic moment for the austenite and martensite is almost unchanged in the $Ni_2Mn_{1.5-x}Cu_xTi_{0.5}$ and $Ni_{2-y}Co_yMn_{1.5-x}Cu_xTi_{0.5}$ ($y < 0.625$) series. However, the austenite total magnetic moment suddenly increases in the $Ni_{2-y}Co_yMn_{1.5-x}Cu_xTi_{0.5}$ ($y = 0.625$) series and gradually reduces with the increase of Cu content, which is mainly due to that the paramagnetic Cu substitutes ferromagnetic Mn, while the magnetism is mainly contributed by Mn atoms [40–44].

Besides, the Mn moments are arranged in antiparallel with high symmetry in the $Ni_2Mn_{1.5-x}Cu_xTi_{0.5}$ and $Ni_{2-y}Co_yMn_{1.5-x}Cu_xTi_{0.5}$ ($y < 0.625$) series, while parallel alignment in the austenite of the $Ni_{2-y}Co_yMn_{1.5-x}Cu_xTi_{0.5}$ ($y = 0.625$) series, leading to a sudden increase in the total magnetic moment. The above results are the same as that of E_{form}.

3.3. Electronic structures

The electronic density of states (DOS) of the $Ni_{2-y}Co_yMn_{1.5-x}Cu_xTi_{0.5}$ ($x = 0.125, 0.25, 0.375$, $y = 0, 0.625$) series was studied in detail in order to study the essence of the mechanical and magnetic properties.

The total DOS of the martensite and austenite for the $Ni_2Mn_{1.5-x}Cu_xTi_{0.5}$ and $Ni_{1.375}Co_{0.625}Mn_{1.5-x}Cu_xTi_{0.5}$ series is shown in Fig. 5. The total DOS of the AFA and AFM phases have very high symmetry for the Cu1, Cu2, and Cu3 alloys according to Fig. 5(a), (c), and (e), which illustrates that their total magnetic moments are almost zero. However, for the Cu1Co5, Cu2Co5, and Cu3Co5 alloys as seen in Fig. 5(b), (d), and (f), the total DOS for the AFM phase has a high symmetry, while that of the FA phase possesses a relatively low symmetry. Such electronic structures provide explanation for the magnetic change of the austenite with Co doping.

The partial DOS of the $Ni_2Mn_{1.5-x}Cu_xTi_{0.5}$ and $Ni_{1.375}Co_{0.625}Mn_{1.5-x}Cu_xTi_{0.5}$ ($x = 0.125, 0.25, 0.375$) series is displayed in Fig. 6. Fig. 6(a)–(c) shows that the up-spin and down-spin parts of the Ni, Mn, and Cu 3d DOS have hybridization effect under the Fermi level (E_F). Meanwhile, the 3d Ni and Mn partial DOS exist hybridization effect within the energy range of −3.4 to −0.7 eV. The Cu and Mn partial DOS have strong hybridization effect around −3.2 and −1.5 eV. Strong d–d hybridization is closely related to the enhancement of ductility [18,37]. The partial DOS is symmetric and opposite, which indicates that Ni, Ti, and Cu magnetic moments are close to zero, in addition, the Mn_{Mn} and Mn_{Ti} partial DOS cancel each other out, so the total magnetic moment approaches zero.

The situation is different for the Co doping case, the up-spin and down-spin Ni, Mn, Ti, Co, and Cu partial 3d DOS are asymmetric, as shown in Fig. 6(d)–(f). Based on the electronic structures, it reasonably explains that the austenite is antiferromagnetic in the $Ni_2Mn_{1.5-x}Cu_xTi_{0.5}$ series, but ferromagnetic state in the $Ni_{1.375}Co_{0.625}Mn_{1.5-x}Cu_xTi_{0.5}$ series.

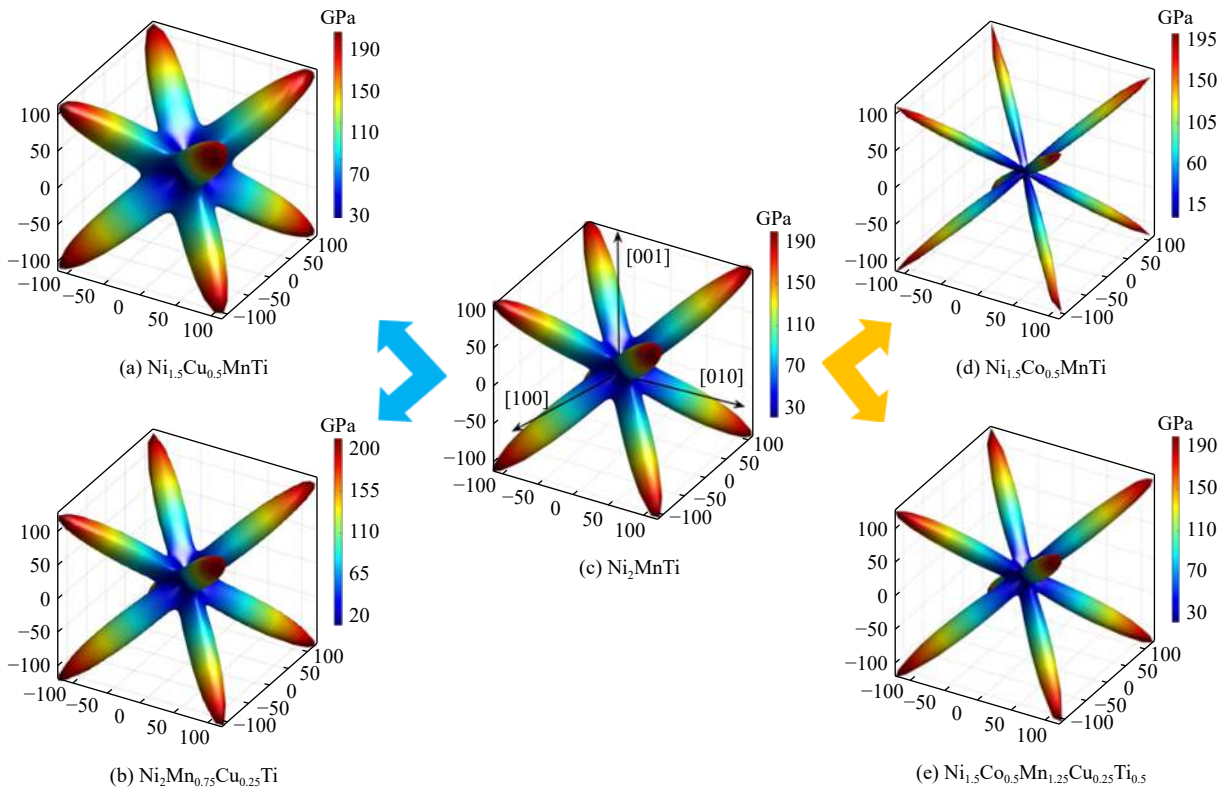

Fig. 3. Three-dimensional Young's modulus for single-crystal (a) $Ni_{1.5}Cu_{0.5}MnTi$, (b) $Ni_2Mn_{0.75}Cu_{0.25}Ti$, (c) Ni_2MnTi, (d) $Ni_{1.5}Co_{0.5}MnTi$, and (e) $Ni_{1.5}Co_{0.5}Mn_{1.25}Cu_{0.25}Ti_{0.5}$ alloys.

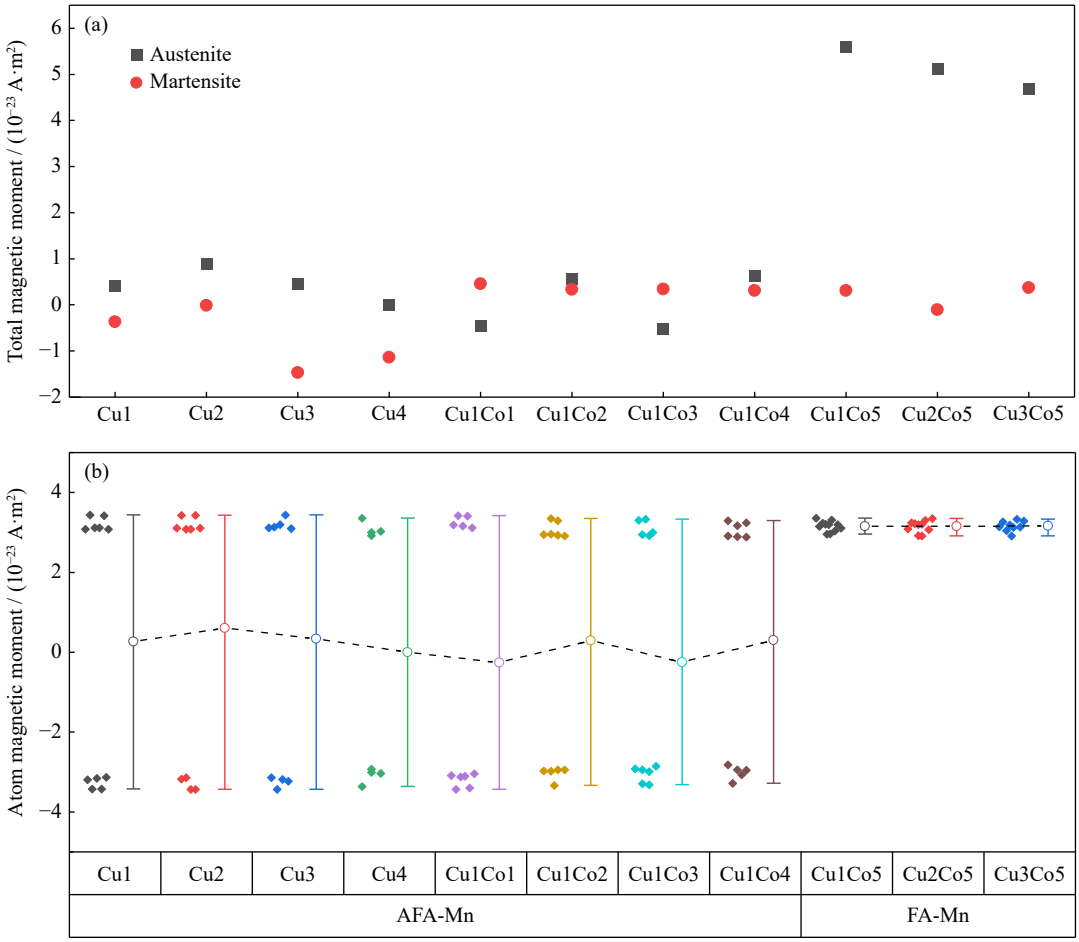

Fig. 4. (a) Total magnetic moments of austenite and martensite and (b) atomic magnetic moments of Mn in austenite for $Ni_2Mn_{1.5-x}Cu_xTi_{0.5}$ (x = 0.125, 0.25, 0.375 and 0.5) and $Ni_{2-y}Co_yMn_{1.5-x}Cu_xTi_{0.5}$ [(x = 0.125, y = 0.125, 0.25, 0.375, 0.5) and (x = 0.125, 0.25, 0.375, y = 0.625)] series.

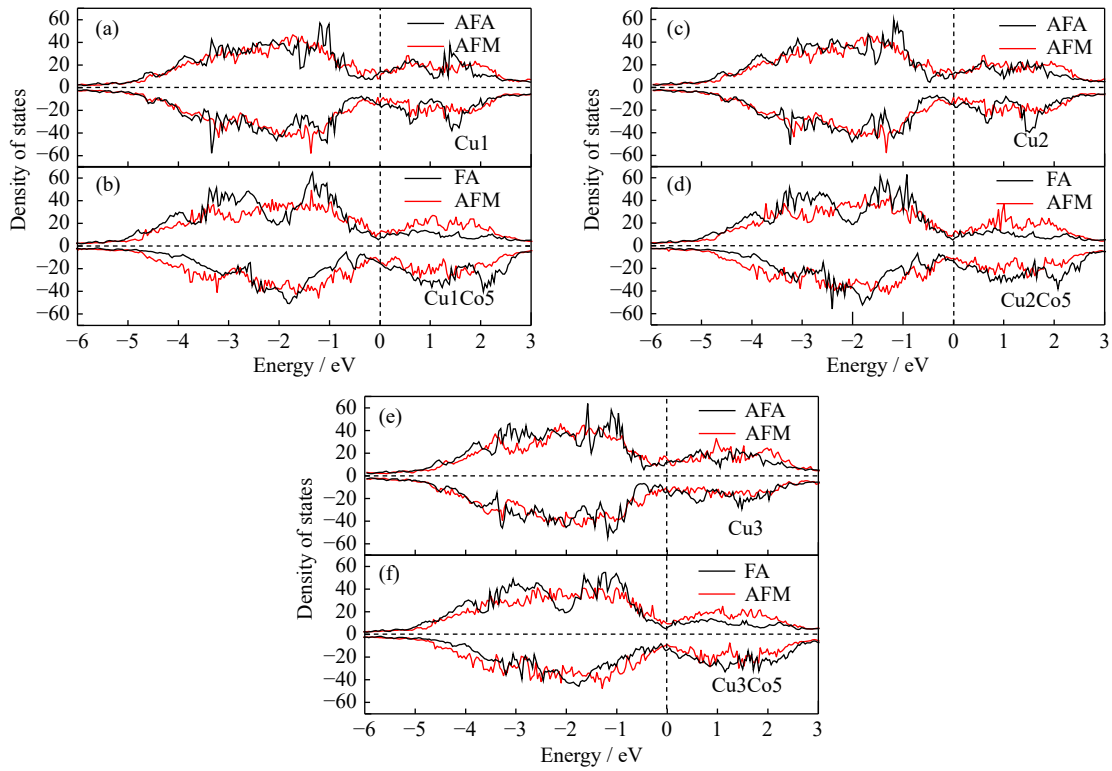

Fig. 5. Total electronic density of states of austenite and martensite for (a, c, e) $Ni_2Mn_{1.5-x}Cu_xTi_{0.5}$ (x = 0.125, 0.25, 0.375) and (b, d, f) $Ni_{1.375}Co_{0.625}Mn_{1.5-x}Cu_xTi_{0.5}$ (x = 0.125, 0.25, 0.375) series.

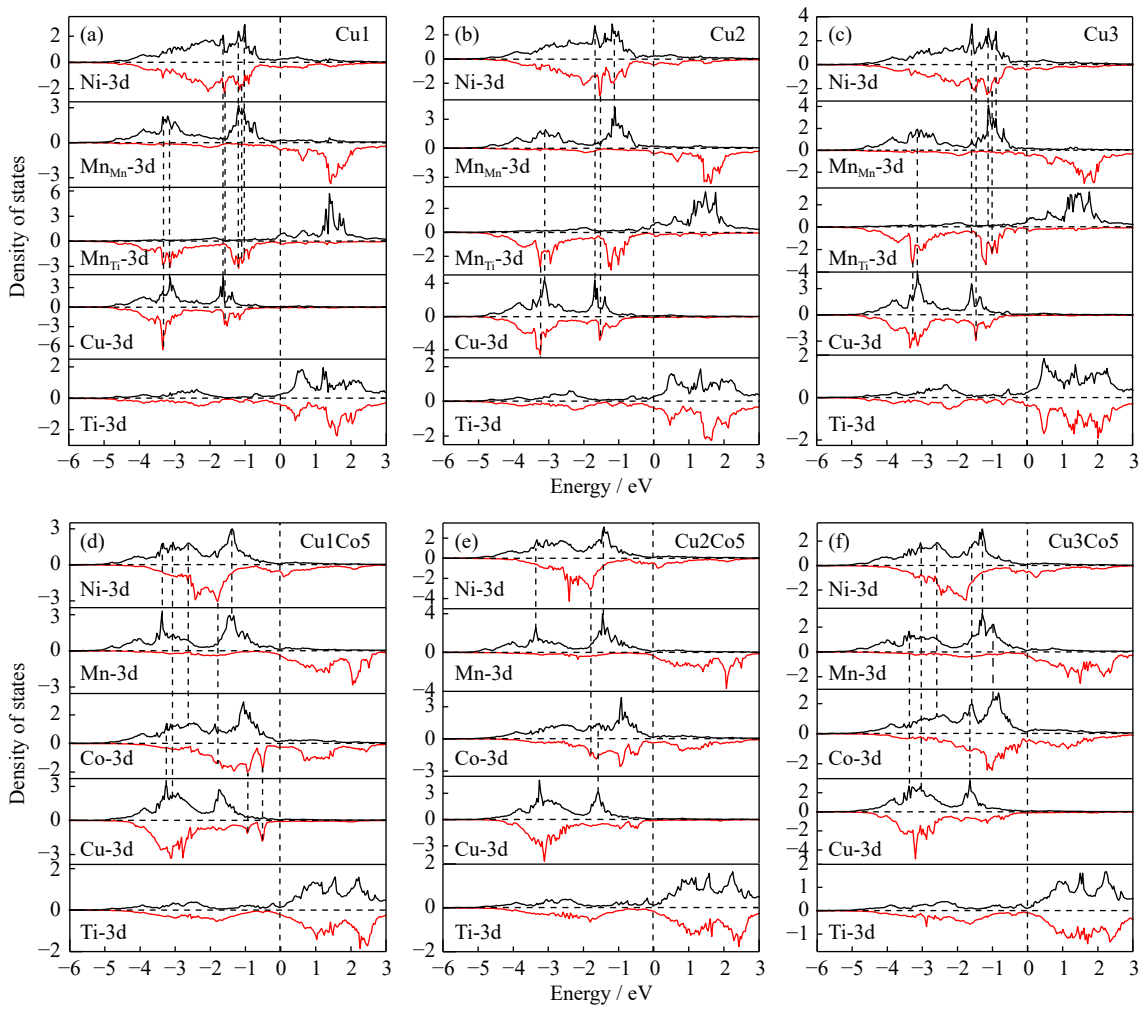

Fig. 6. Partial density of states of austenite for (a, b, c) $Ni_2Mn_{1.5-x}Cu_xTi_{0.5}$ (x = 0.125, 0.25, 0.375) and (d, e, f) $Ni_{1.375}Co_{0.625}Mn_{1.5-x}Cu_xTi_{0.5}$ (x = 0.125, 0.25, 0.375) series.

4. Conclusions

The first-principles calculations for the martensitic transformation, mechanical and magnetic properties for $Ni_2Mn_{1.5-x}Cu_xTi_{0.5}$ (x = 0.125, 0.25, 0.375, 0.5) and $Ni_{2-y}Co_yMn_{1.5-x}Cu_xTi_{0.5}$ [(x = 0.125, y = 0.125, 0.25, 0.375, 0.5) and (x = 0.125, 0.25, 0.375, y = 0.625)] alloys are investigated in this paper. The main results are as follows.

For the formation energy, the martensite is smaller than the austenite, all the investigated Ni–(Co)–Mn–Cu–Ti alloys will undergo martensitic transformation. The martensite and austenite for the $Ni_2Mn_{1.5-x}Cu_xTi_{0.5}$ and $Ni_{2-y}Co_yMn_{1.5-x}Cu_xTi_{0.5}$ (y < 0.625) alloys always exist in an antiferromagnetic state and the total magnetic moments are almost zero, but the austenite of the $Ni_{2-y}Co_yMn_{1.5-x}Cu_xTi_{0.5}$ (y = 0.625) alloys exists in ferromagnetic state. Cu doping reduces thermal hysteresis and anisotropy for the Ni–(Co)–Mn–Ti alloy. Increasing Mn and decreasing Ti content in the Ni–Mn–Cu–Ti alloy can improve the shear resistance and normal stress resistance, but reduce the toughness. The Ni–Mn–Cu–Ti and Ni–Co–Mn–Ti alloys have a relatively larger value of P_c, B/G, and ν. The ductility of the $Ni_{1.5}Co_{0.5}MnTi$ alloy is stronger than that of the Ni–Mn–Cu–Ti alloy, while the ductility of the Ni–Co–Mn–Cu–Ti alloy is inferior to that of the Ni–Mn–Cu–Ti and Ni–Co–Mn–Ti alloys. Besides, Co, Cu doping, and Cu–Co co-doping can reduce the incompressibility and ductility of the Ni–Mn–Ti-based alloys.

Acknowledgements

This work was financially supported by the National Natural Science Foundation of China (No. 51771044), the Natural Science Foundation of Hebei Province (No. E2019501061), the Performance subsidy fund for Key Laboratory of Dielectric and Electrolyte Functional Material Hebei Province (No. 22567627H), the Fundamental Research Funds for the Central Universities (No. N2223025), the State Key Lab of Advanced Metals and Materials (No. 2022-Z02), and Programme of Introducing Talents of Discipline Innovation to Universities 2.0 (the 111 Project of China 2.0, No. BP0719037). This work was carried out at Shanxi Supercomputing Center of China, and the calculations were performed on TianHe-2.

Conflict of Interest

The authors declare no potential conflict of interest.

References

[1] M. Callisti and T. Polcar, Microstructural evolution of nanometric $Ti(NiCu)_2$ precipitates in annealed Ni–Ti–Cu thin films, *Vacuum*, 117(2015), p. 1.

[2] D.Y. Cong, W.X. Xiong, A. Planes, *et al*., Colossal elastocaloric effect in ferroelastic Ni–Mn–Ti alloys, *Phys. Rev. Lett.*, 122(2019), No. 25, art. No. 255703.

[3] J.D. Navarro-García, J.L. Sánchez Llamazares, and J.P.Camarillo-Garcia, Synthesis of highly dense spark plasma sintered magnetocaloric Ni–Mn–Sn alloys from melt-spun ribbons, *Mater. Lett.*, 295(2021), art. No. 129857.

[4] W.T. Chiu, P. Sratong-on, M. Tahara, V. Chernenko, and H. Hosoda, Large magnetostrains of Ni–Mn–Ga/silicone composite containing system of oriented 5M and 7M martensitic particles, *Scripta Mater.*, 207(2022), art. No. 114265.

[5] J. Liu, T. Gottschall, K.P. Skokov, J.D. Moore, and O. Gutfleisch, Giant magnetocaloric effect driven by structural transitions, *Nat. Mater.*, 11(2012), No. 7, p. 620.

[6] A. Biesiekierski, J.X. Lin, Y.C. Li, D.H. Ping, Y. Yamabe-Mitarai, and C.E. Wen, Impact of ruthenium on mechanical properties, biological response and thermal processing of β-type Ti–Nb–Ru alloys, *Acta Biomater.*, 48(2017), p. 461.

[7] X.L.Yang and J.X. Shang, Electronic mechanism of martensitic transformation in Nb-doped NiTi alloys: A first-principles investigation, *ACS Omega*, 6(2021), No. 34, p. 22033.

[8] R. Kainuma, Y. Imano, W. Ito, *et al*., Magnetic-field-induced shape recovery by reverse phase transformation, *Nature*, 439(2006), No. 7079, p. 957.

[9] S.Y. Yu, Z.X. Cao, L. Ma, *et al*., Realization of magnetic field-induced reversible martensitic transformation in NiCoMnGa alloys, *Appl. Phys. Lett.*, 91(2007), No. 10, art. No. 102507.

[10] M. Wuttig, L. Liu, K. Tsuchiya, and R.D. James, Occurrence of ferromagnetic shape memory alloys (invited), *J. Appl. Phys.*, 87(2000), No. 9, p. 4707.

[11] J.A. Monroe, I. Karaman, B. Basaran, *et al*., Direct measurement of large reversible magnetic-field-induced strain in Ni–Co–Mn–In metamagnetic shape memory alloys, *Acta Mater.*, 60(2012), No. 20, p. 6883.

[12] F.X. Hu, B.G. Shen, J.R. Sun, and G.H. Wu, Large magnetic entropy change in a Heusler alloy $Ni_{52.6}Mn_{23.1}Ga_{24.3}$ single crystal, *Phys. Rev. B*, 64(2001), No. 13, art. No. 132412.

[13] J. Du, Q. Zheng, W.J. Ren, W.J. Feng, X.G. Liu, and Z.D. Zhang, Magnetocaloric effect and magnetic-field-induced shape recovery effect at room temperature in ferromagnetic Heusler alloy Ni–Mn–Sb, *J. Phys. D: Appl. Phys.*, 40(2007), No. 18, p. 5523.

[14] G.Y. Zhang, D. Li, C. Liu, *et al*., Giant low-field actuated caloric effects in a textured $Ni_{43}Mn_{47}Sn_{10}$ alloy, *Scripta Mater.*, 201(2021), art. No. 113947.

[15] H. Wang, D. Li, G. Zhang, *et al*., Highly sensitive elastocaloric response in a directionally solidified $Ni_{50}Mn_{33}In_{15.5}Cu_{1.5}$ alloy with strong A preferred orientation, *Intermetallics*, 140(2022), art. No. 107379.

[16] Y.J. Huang, Q.D. Hu, N.M. Bruno, *et al*., Giant elastocaloric effect in directionally solidified Ni–Mn–In magnetic shape memory alloy, *Scripta Mater.*, 105(2015), p. 42.

[17] Z.Y. Wei, W. Sun, Q. Shen, *et al*., Elastocaloric effect of all-d-metal Heusler NiMnTi(Co) magnetic shape memory alloys by digital image correlation and infrared thermography, *Appl. Phys. Lett.*, 114(2019), No. 10, art. No. 101903.

[18] H.L. Yan, L.D. Wang, H.X. Liu, *et al*., Giant elastocaloric effect and exceptional mechanical properties in an all-d-metal Ni–Mn–Ti alloy: Experimental and ab-initio studies, *Mater. Des.*, 184(2019), art. No. 108180.

[19] Z.Y. Wei, E.K. Liu, J.H. Chen, *et al*., Realization of multifunctional shape-memory ferromagnets in all-d-metal Heusler phases, *Appl. Phys. Lett.*, 107(2015), No. 2, art. No. 022406.

[20] K. Liu, S.C. Ma, C.C. Ma, *et al*., Martensitic transformation and giant magneto-functional properties in all-d-metal Ni–Co–Mn–Ti alloy ribbons, *J. Alloys Compd.*, 790(2019), p. 78.

[21] Z.Q. Guan, X.J. Jiang, J.L. Gu, *et al*., Large magnetocaloric effect and excellent mechanical properties near room temperature in Ni–Co–Mn–Ti non-textured polycrystalline alloys, *Appl. Phys. Lett.*, 119(2021), No. 5, art. No. 051904.

[22] A. Taubel, B. Beckmann, L. Pfeuffer, *et al*., Tailoring magnetocaloric effect in all-d-metal Ni–Co–Mn–Ti Heusler alloys: A combined experimental and theoretical study, *Acta Mater.*, 201(2020), p. 425.

[23] X.Z. Liang, J. Bai, J.L. Gu, *et al*., Probing martensitic transformation, kinetics, elastic and magnetic properties of $Ni_{2-x}Mn_{1.5}In_{0.5}Co$ alloys, *J. Mater. Sci. Technol.*, 44(2020), p. 31.

[24] J. Hafner, Atomic-scale computational materials science, *Acta Mater.*, 48(2000), No. 1, p. 71.

[25] G. Kresse and D. Joubert, From ultrasoft pseudopotentials to the projector augmented-wave method, *Phys. Rev. B*, 59(1999), No. 3, p. 1758.

[26] P.E. Blöchl, Projector augmented-wave method, *Phys. Rev. B*, 50(1994), No. 24, p. 17953.

[27] G. Kern, G. Kresse, and J. Hafner, *Ab initio* calculation of the lattice dynamics and phase diagram of boron nitride, *Phys. Rev. B*, 59(1999), No. 13, p. 8551.

[28] J.P. Perdew, K. Burke, and M.Ernzerhof, Generalized gradient approximation made simple, *Phys. Rev. Lett.*, 77(1996), No. 18, p. 3865.

[29] H.J. Monkhorst and J.D. Pack, Special points for Brillouin-zone integrations, *Phys. Rev. B*, 13(1976), No. 12, p. 5188.

[30] Y. Song, X. Chen, V. Dabade, T.W. Shield, and R.D. James, Enhanced reversibility and unusual microstructure of a phase-transforming material, *Nature*, 502(2013), No. 7469, p. 85.

[31] J. Cui, Y.S. Chu, O.O. Famodu, *et al*., Combinatorial search of thermoelastic shape-memory alloys with extremely small hysteresis width, *Nat. Mater.*, 5(2006), No. 4, p. 286.

[32] Z.G. Wu, Z.H. Liu, H. Yang, Y. Liu, and G. Wu, Effect of Co addition on martensitic phase transformation and magnetic properties of $Mn_{50}Ni_{40-x}In_{10}Co_x$ polycrystalline alloys, *Intermetallics*, 19(2011), No. 12, p. 1839.

[33] Z.B Li, J.J. Yang, D. Li, *et al*., Tuning the reversible magnetocaloric effect in Ni–Mn–In-based alloys through Co and Cu Co-doping, *Adv. Electron. Mater.*, 5(2019), No. 3, art. No. 1800845.

[34] M. Kaya, S. Yildirim, E. Yüzüak, I. Dincer, R. Ellialtioglu, and Y. Elerman, The effect of the substitution of Cu for Mn on magnetic and magnetocaloric properties of $Ni_{50}Mn_{34}In_{16}$, *J. Magn. Magn. Mater.*, 368(2014), p. 191.

[35] S. Saritaş, M. Kaya, İ. Dinçer, and Y. Elerman, The structural, magnetic, and magnetocaloric properties of $Ni_{43}Mn_{46-x}Cu_xIn_{11}$ (x = 0, 0.9, 1.3, and 2.3) Heusler alloys, *Metall. Mater. Trans. A*, 48(2017), No. 10, p. 5068.

[36] Z. Yang, D.Y. Cong, Y. Yuan, *et al*., Large room-temperature elastocaloric effect in a bulk polycrystalline Ni–Ti–Cu–Co alloy with low isothermal stress hysteresis, *Appl. Mater. Today*, 21(2020), art. No. 100844.

[37] Z.Q. Guan, J. Bai, J.L. Gu, *et al*., First-principles investigation of B2 partial disordered structure, martensitic transformation, elastic and magnetic properties of all-d-metal Ni–Mn–Ti Heusler alloys, *J. Mater. Sci. Technol.*, 68(2021), p. 103.

[38] C.C. Xiong, J. Bai, Y.S. Li, *et al*., First-principles investigation on phase stability, elastic and magnetic properties of boron doping in Ni–Mn–Ti alloy, *Acta Metall. Sin. Engl. Lett.*, 35(2022), No. 7, p. 1175.

[39] Z.Q. Guan, J. Bai, Y. Zhang, *et al*., Revealing essence of magnetostructural coupling of Ni–Co–Mn–Ti alloys by first-principles calculations and experimental verification, *Rare Met.*, 41(2022), No. 6, p. 1933.

[40] Z. Muthui, R. Musembi, J. Mwabora, and A. Kashyap, Perpendicular magnetic anisotropy in nearly fully compensated ferrimagnetic Heusler alloy $Mn_{0.75}Co_{1.25}VIn$: An *ab initio* study, *J. Magn. Magn. Mater.*, 442(2017), p. 343.

[41] R.V.S. Prasad, M. Manivel Raja, and G. Phanikumar, Microstructure and magnetic properties of rapidly solidified Ni_2(Mn,Fe)Ga Heusler alloys, *Adv. Mater. Res.*, 74(2009), p. 215.

[42] Z.N. Ni, X.M. Guo, X.T. Liu, Y.Y, Jiao, F.B. Meng, and H.Z. Luo, Understanding the magnetic structural transition in all-d-metal Heusler alloy $Mn_2Ni_{1.25}Co_{0.25}Ti_{0.5}$, *J. Alloys Compd.*, 775(2019), p. 427.

[43] J. Bai, J.M. Raulot, Y.D. Zhang, C. Esling, X. Zhao, and L. Zuo, Crystallographic, magnetic, and electronic structures of ferromagnetic shape memory alloys Ni_2XGa (X = Mn, Fe, Co) from first-principles calculations, *J. Appl. Phys.*, 109(2011), No. 1, art. No. 014908.

[44] J. Bai, J.L. Wang, S.F. Shi, *et al*., Complete martensitic transformation sequence and magnetic properties of non-stoichiometric $Ni_2Mn_{1.2}Ga_{0.8}$ alloy by first-principles calculations, *J. Magn. Magn. Mater.*, 473(2019), p. 360.